



# Information flow, gating, and energetics in dimeric molecular motors

Ryota Takaki<sup>a,1</sup>, Mauro L. Mugnai<sup>b,2</sup>, and D. Thirumalai<sup>c,3</sup>

Edited by Anatoly Kolomeisky, Rice University, Houston, TX; received May 10, 2022; accepted September 26, 2022 by Editorial Board Member Yale E. Goldman

Molecular motors, kinesin and myosin, are dimeric consisting of two linked identical monomeric globular proteins. Fueled by the free energy generated by ATP hydrolysis, they walk on polar tracks (microtubule or filamentous actin) processively, which means that only one head detaches and executes a mechanical step while the other stays bound to the track. One motor head must regulate the chemical state of the other, referred to as "gating", a concept that is still not fully understood. Inspired by experiments, showing that only a fraction of the energy from ATP hydrolysis is used to advance the kinesin motors against load, we demonstrate that the rest of the energy is associated with chemical transitions in the two heads. The coordinated chemical transitions involve communication between the two heads - a feature that characterizes gating. We develop a general framework, based on information theory and stochastic thermodynamics, and establish that gating could be quantified in terms of information flow between the motor heads. Applications to kinesin-1 and Myosin V show that information flow, with positive cooperativity, at external resistive loads less than a critical value,  $F_c$ . When force exceeds  $F_c$ , effective information flow ceases. Interestingly,  $F_c$ , which is independent of the input energy generated through ATP hydrolysis, coincides with the force at which the probability of backward steps starts to increase. Our findings suggest that transport efficiency is optimal only at forces less than  $F_c$ , which implies that these motors must operate at low loads under in vivo conditions.

molecular motor | stochastic thermodynamics | information flow | gating

Molecular motors utilize chemical energy released by ATP hydrolysis in order to carry out multiple cellular functions that include transportation of vesicles (1-3). Dimeric cytoplasmic motors (kinesin and myosin), constructed from two identical ATPases referred to as motor heads, walk on polar tracks (F-actin or microtubule [MT]) by a hand-overhand mechanism (Fig. 1A) (4-6). In order for dimeric motors to take multiple steps in the forward direction, without disengaging from the polar track, there has to be coordination or communication between the motor heads. This implies that the trailing head (TH) should detach with substantially higher probability than the leading head (LH) (a manifestation of interhead communication), while the LH should remain strongly bound to the polar track. Because the nucleotide state (for example, ATP bound or ADP bound) of the motor heads dictates the affinity for the polar track, it follows that the ATPase cycle in the TH and LH should be partially out of phase (7) to ensure effective interhead communication. In kinesin-1 (Kin-1), ATP binds to the LH only after the ADPbound TH detaches from the MT (8–10). In myosin V, interhead communication results from faster ADP release from the TH than from the LH (11, 12). Thus, chemical state (CS) regulation of one motor head by the other plays a significant role in the ability of the motor to take multiple steps on the polar track. This is referred to as "gating," which may be viewed as a form of allosteric regulation (13), in molecular motors. Gating, which is necessary for dimeric motors to maintain processivity, is possibly mediated by interhead mechanical strain through the structural elements connecting the two heads (14-25). Decrease in the gating efficiency in artificial constructs that mutate these elements (for example, elongation of the neck linker in conventional kinesin) results in the reduction of velocity and run length, and a decrease in the stall force (15, 19, 20, 24). From these observations, we surmise that communication between the dimeric motors must be directly linked to energy costs needed to drive stepping.

In order to describe gating, we lean on the thermodynamics of small systems, termed stochastic thermodynamics (26, 27). Unlike conventional thermodynamics, where thermal noise is negligible in the thermodynamic limit, stochastic thermodynamics describes the energetics where the relevant energy scale is comparable to thermal energy. Molecular machines operate in such an environment, and thus the language of stochastic thermodynamics is appropriate to investigate the thermodynamics of molecular motors. In this

## **Significance**

Two-headed kinesin and myosin are motor proteins, which shuttle cargo in cells by taking multiple steps on microtubules and actin, respectively. In executing multiple steps, one head is always bound to the polar track. Despite tremendous progress made over the years, the mechanism by which the two heads communicate ("gating"), thus ensuring that one head is always bound, is not fully understood. We provide a quantitative description of the gating mechanism, using information theory and stochastic thermodynamics. Information flow for kinesin-1 and myosin V is qualitatively similar, which is manifested by the decrease in the efficacy of gating at a critical external load on the motor. Our finding suggests a universal mechanism of gating for dimeric molecular motors.

Author contributions: R.T. and D.T. designed research; R.T., M.L.M., and D.T. performed research; D.T. contributed new reagents/analytic tools; R.T., M.L.M., and D.T. analyzed data; and R.T., M.L.M., and D.T. wrote the paper.

The authors declare no competing interest.

This article is a PNAS Direct Submission. A.K. is a guest editor invited by the Editorial Board.

Copyright © 2022 the Author(s). Published by PNAS. This article is distributed under Creative Commons Attribution-NonCommercial-NoDerivatives License 4.0 (CC BY-NC-ND).

<sup>1</sup>Present address: Max Planck Institute for the Physics of Complex Systems, Nöthnitzer Str.38, 01187 Dresden,

<sup>2</sup>Present address: Institute for Soft Matter Synthesis and Metrology Georgetown University, Washington, DC 20057

 $^3\text{To}$  whom correspondence may be addressed. Email: dave.thirumalai@gmail.com.

This article contains supporting information online at https://www.pnas.org/lookup/suppl/doi:10.1073/pnas. 2208083119/-/DCSupplemental.

Published November 7, 2022.

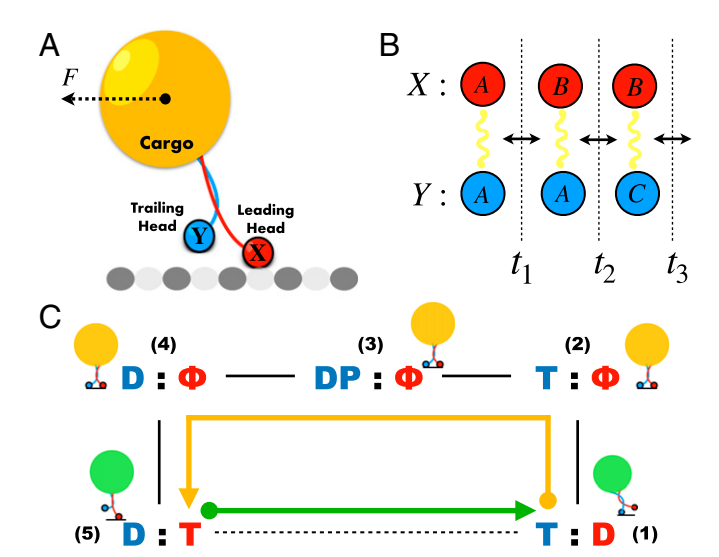


Fig. 1. Kinesin stepping and associated transitions. (A) Schematics of a typical optical trap experiment used to monitor stepping on the MT. A resistive force, F, acts on the cargo. (B) Example of transitions for interacting systems with X and Y being the leading and trailing heads, respectively. The CSs associated with X and Y are denoted by circled letters A, B, and C. In this example, the transition in X is described as  $(x_0, y_0) = (A, A) \longrightarrow (x_1, y_0) = (B, A)$ , and the transition in Y is given by  $(x_1, y_0) = (B, A) \longrightarrow (x_1, y_1) = (B, C)$ . Transitions occur at times  $t_1, t_2, t_3, \cdots$ . (C) Forward stepping cycle for kinesin. The cycle is divided into CS transitions (yellow) and mechanical stepping (green). The CS of the TH is in blue, and that of the LH is shown in red. The nucleotide state T denotes ATP, Φ means the nucleotide state is not bound, D denotes ADP, and DP is the post hydrolyzed state with the trailing containing ADP plus the inorganic phosphate, Pi. The caricatures for the physical states of the motor corresponding to each CS are displayed.

formulation, which we exploit here, entropy production is an essential element (28, 29). In particular, mutual information (MI) characterizes the correlations between two variables and can be treated on the same footing as work and free energy (30-33), an insight that is the basis of our work.

The importance of information theory in biology has been previously recognized. For example, information transduction in the adaptive sensory system and description of molecular motors from the perspective of information storage have been investigated (34-38). More recently, Lathouwers and Sivak (39) examined power and information transduction in F<sub>0</sub>F<sub>1</sub>-ATP synthase, and Amano et al. (40) studied an artificial chemical nanomachine driven by an information ratchet. Our goal here is to use information transfer between the heads of dimeric motors as the basis of communication—an issue that has not been considered before. We build on the previous studies and develop a framework, based on stochastic network models, to quantify gating in terms of information theory.

We were motivated to cast gating in light of information theory because astounding developments in experimental techniques have made it possible to measure energetics in molecular motors with high accuracy (33, 41). In a recent single-molecule experiment, Ariga et al. (41) measured energetics of kinesin by attaching a probe to the motor. The experiments produced two important results. 1) They established that the motor functions out of equilibrium by showing that the relation between response and correlation function, expected for a system at equilibrium, does not hold. The extent of violation of the fluctuation response relation was quantified by using the Harada-Sasa equality (42, 43). 2) Based on the experimental data and a theoretical model, it was suggested (41) that the total heat dissipated is  $\approx$ 80% of the input energy, which implies that only  $\approx$ 20% of the energy from ATP hydrolysis is utilized in performing work.

Our theory is based on stochastic network models. We assume that, in the process stepping along the cytoskeletal filament, the dimeric motor could be driven into a nonequilibrium steady state (NESS) (26, 29, 44-48), provided that it does not detach from the polar track. The present work, which provides a framework for understanding gating in cytoplasmic motors in terms of information flow, utilizes and builds on the most insightful formulation by Horowitz and Esposito (49). In the process, we establish precise connections between interhead communication and energetics in dimeric motors. Although we only consider stepping in Kin-1 and myosin V, our approach is general, and could be used to understand gating and energy costs in other molecular machines (29). We show that the energy costs involved in the operation of the motors is related to information flow (gating) between the motor heads.

## **Theory**

Notations and Assumptions. We consider two subsystems, labeled X and Y (49), which, in the context of molecular motors, represent the LH and the TH, respectively. Each subsystem is specified by microstates x and y (Fig. 1B). A pair of states associated with X and Y is labeled (x, y). We restrict ourselves to a network connecting (x, y) that is bipartite, which means that only X or Y can alter its state in a single transition. In other words, the transitions  $(x_1, y_1) \rightarrow (x_2, y_1)$  and  $(x_1, y_1) \rightarrow$  $(x_1, y_2)$  are allowed, but not  $(x_1, y_1) \rightarrow (x_2, y_2)$ , with  $x_1 \neq x_2$ and  $y_1 \neq y_2$ . However, we require the bipartite structure only along the path in which we calculate the interaction between X and Y. A nonbipartite feature, which is needed in describing stepping in molecular motors, is allowed otherwise.

Consider the chemomechanical cycle of Kin-1 in Fig. 1C. First, let us divide the whole chemomechanical cycle of the motor into chemical and mechanical processes, and then introduce bipartite constraints only on the chemical process. TH in blue and LH in red are the two subsystems transitioning between the CSs [(1)  $\rightarrow$ (5); yellow arrow] maintains the bipartite structure. However, the mechanical steps ((5)  $\rightarrow$  (1); green arrow), that result in switching of the positions of the two heads, exchange the roles of LH and TH. Thus, mechanical steps are nonbipartite.

We describe the properties of the motor in the steady state using the joint probability p(x,y) for the state (x,y), and the marginal probabilities for X and Y,  $p_X(x) = \sum_y p(x,y)$  and  $p_Y(y) = \sum_x p(x, y)$ , respectively. We set the temperature T to unity, unless specified.

Information Flow on CS Transitions. The point-wise MI (PMI), which plays an important role in this study, in the energy unit, i(x, y), for a state (x, y), is

$$i(x,y) = k_B \ln \frac{p(x,y)}{p_X(x)p_Y(y)},$$
 [1]

where  $k_B$  is the Boltzmann constant. It is necessary to introduce PMI, instead of considering only the MI, because information flow in motors requires quantifying the microscopic transitions in each step in the catalytic cycle (Fig. 1C). The MI is the average over all the states,  $\sum_{x,y} p(x,y) i(x,y)$ .

One can compute the change of PMI between two arbitrary states. We define the change of PMI from the state  $(x_0, y_0)$  to  $(x_n,y_n)$  as

$$\Delta i \equiv i(x_n, y_n) - i(x_0, y_0).$$
 [2]

For a bipartite path, Eq. 2 has a clear interpretation:  $\Delta i$ quantifies the net information transferred between X and Y along the transitions. We show the computation of  $\Delta i$  for a bipartite path in Information Flow on Chemical State Transitions in the Methods section.

We are interested in how the input energy, arising from ATP hydrolysis, is parsed into the "invisible" CS transitions (from (1) to (5) in the catalytic cycle in Fig. 1*C*), and the mechanical transition  $((5) \rightarrow (1) \text{ in Fig. } 1C)$ . Therefore, it is the information flow along a specific path (for instance,  $(2) \rightarrow (3)$  in Fig. 1C), rather than information flow in the closed cycle (transition starting in (1) and ending in (1), resulting in the LH and TH switching positions on the polar track) that is relevant for gating. In contrast, for different reasons, previous studies (39, 49-51) focused on the information flow using the MI. Therefore, information flow of interest in these studies is restricted to a closed cycle in which all the edges in the network are bipartite. As a result, the net information transfer between two subsystems is zero in NESS. In Eq. 2, the net information flow between two subsystems need not be zero along a specific path but vanishes only when we compute the information flow for a closed path. In molecular motors, we need to quantify heat dissipation along the invisible CS transitions. For this reason, we calculate path or transition specific energy cost for a fixed input

**Entropy Production and Information Flow.** Entropy production,  $\rho$ , plays a central role in nonequilibrium systems, quantifying the deviation from the equilibrium. In bipartite systems, it is possible to derive a simple equality connecting the entropy production and information flow (Eq. 2). We delegate the derivation to Entropy Production and Information Flow. The relation reads

$$\rho = \sigma - \Delta i.$$
 [3]

 $\sigma$  is the apparent entropy production, quantifying the dissipation when we do not take into account the communication (correlation) between the two variables. In the context of dimeric motors,  $\sigma$  is the dissipation from the motor when we do not take into account the effect of the gating mechanism. When there is no communication between the two motor heads ( $\Delta i = 0$ ),  $\sigma$ coincides with  $\rho$ .

The entropy production,  $\rho$ , is always positive in the direction of stationary flow. Therefore, the lower bounds for the apparent entropy production are  $\Delta i$ . The value of  $\sigma$  is allowed to be negative provided  $\Delta i \leq \sigma$ . Negative values might be indicative of an apparent violation of the second law of thermodynamics, and are sometimes taken to be a signature of a Maxwell demon (49, 52-54). We discuss the Maxwell demon regime (MDR) further below.

Free-Energy Transduction and Information. We consider an isothermal environment at temperature T with the possibility that material exchange occurs, resulting in the breakdown of the detail balance condition. In the context of molecular motors, this is realized by maintaining the concentrations of the ligands (ATP, ADP, phosphate  $[P_i]$ ) at constant values (46). For the chemical transition network in the NESS, it is possible to identify the chemical free-energy transduction with the entropy production along the path connecting any two states (55). This, in turn, allows us to compute the free-energy transduction  $(\Delta \mu)$  using the entropy production along the path:  $\Delta \mu = \rho$ . We note that the same concept is formulated in terms of energy balance condition (56). If the CS transitions are driven by ATP hydrolysis generating energy input  $\Delta\mu$ , then the free-energy transduction for the cyclic CS transition path (initial and final state is identical) is

 $\Delta \mu = \rho = Q$ , where Q is the heat dissipated during the cycle. In general, however, the starting and ending states do not necessarily coincide. In such cases,  $\rho$  should include not only Q but also the difference in the internal energy.

It is clear from Eq. 3 that the free-energy transduction in the motors may be written, using the apparent entropy production and the associated information flow terms, as

$$\Delta \mu = \sigma - \Delta i.$$
 [4]

The equation above relates the free-energy transduction during the CS transitions and information operation associated with coordination between the two heads in the dimeric motors. If there is no interaction or communication between the two motor heads ( $\Delta i = 0$ ), the total free-energy cost would simply be given as the sum of the expenses from each motor head. How the informational term relates to the energetics and mechanical aspects of the motor follows in the analysis given below.

Mechanochemistry and Information. We first illustrate the connection between  $\Delta i$  and motor movement using kinesin as an example. We model the forward stepping cycle for kinesin using the kinetic network shown in Fig. 1C. Completion of a single step (cycle) begins by releasing ADP from the LH  $((1) \rightarrow (2))$ , followed by ATP hydrolysis in the TH  $((2) \rightarrow (3))$ , release of  $P_i$  ((3)  $\rightarrow$  (4)), and ATP binding to the LH ((4)  $\rightarrow$  (5)). The four chemical transitions poise the TH to take a mechanical step  $((5) \rightarrow (1))$ . The catalytic cycle in Fig. 1C naturally decomposes into CS transitions (state (1) to state (5)) ( $\Pi_{ch}$ ) that alter the nucleotide states of the motor, and the mechanical stepping (state (5) to state (1)) ( $\Pi_{mc}$ ). Once mechanical stepping is complete, the next cycle of chemical transitions initiates. We here present the main consequences of the theory applied to the kinetic network in Fig. 1 C. See Mechanochemistry and Information for more-detailed

In anticipation of the link between information flow and gating, we begin with energy conservation associated with the cycle in Fig. 1C. The motor operates by input of energy,  $\Delta \mu$ , arising from ATP hydrolysis. We partition this energy into two contributions:  $\Delta \mu_{ch}$ , associated with the chemical transitions, and the energy  $\Delta \mu_{mc}$  expended in the mechanical step, which advances the motor along the MT by one step (≈8 nm for kinesin). Conservation of energy implies

$$\Delta \mu = \Delta \mu_{ch} + \Delta \mu_{mc}.$$
 [5]

 $\Delta\mu$ ,  $\Delta\mu_{ch}$ , and  $\Delta\mu_{mc}$  can be written using the microscopic rates in the kinetic diagram (*Methods*). Applying Eq. 4 to  $\Pi_{ch}$ , we obtain

$$\Delta\mu_{ch} = \sigma_{ch} - \Delta i_{ch}, \qquad [6]$$

where  $\sigma_{ch}$  and  $\Delta i_{ch}$  are the apparent entropy production and the change of PMI in  $\Pi_{ch}$ , respectively. By conservation of the energy (Eq. 5),

$$\Delta \mu_{mc} = \Delta \mu - \sigma_{ch} + \Delta i_{ch}.$$
 [7]

Eq. 7 quantifies the following physical intuition. The energy that the motor can spend for the mechanical steps  $(\Delta \mu_{mc})$ is the total energy minus the dissipation  $(\Delta \mu - \sigma_{ch})$  plus the correlation developed in  $\Pi_{ch}$  ( $\Delta i_{ch}$ ). The flux of the mechanical stepping,  $J_{mc}$ , is written as

$$J_{mc} = p_1 w_{15} (e^{(\Delta \mu_{mc} - W)/k_B} - 1),$$
 [8]

where W is the work done by the motor,  $p_1$  is the probability in state 1, and  $w_{15}$  is the transition rate from state 1 to state 5. From Eqs. 7 and **8**, it follows that, when  $\Delta i_{ch} > 0$ , the flux  $J_{mc}$  in  $\Pi_{mc}$  increases. This implies that, by increasing  $\Delta i_{ch}$ , more energy ( $\Delta \mu_{mc}$ ) would be available during the mechanical step (see Eq. 7). Therefore, positive  $\Delta i_{ch} > 0$  implies that the communication between the heads is efficient, a situation that we refer to as positive cooperativity. In contrast, when  $\Delta i_{ch} < 0$  (negative cooperativity), the motor has to expend  $\Delta i_{ch}$  in addition to  $\sigma_{ch}$  to execute the chemical transitions in order to complete the cycle (see Eq. **6**), that is, maintaining coordination costs additional energy for  $\Delta i_{ch} < 0$ . This results in a decrease in the available energy for carrying out the mechanical step (see Eq. 7). Therefore, we surmise that information flow  $\Delta i_{ch}$  quantifies the efficacy of gating in dimeric motors.

Expressions for the key quantities using the steady-state probability, such as  $\Delta i_{ch}$ , for the kinetic network in Fig. 1C are given in *SI Appendix*, section I.

#### **Kinesin**

By using our theory, we first analyzed the energetics and information flow in the forward stepping cycle of Kin-1 using the experimental data (41). The implementation of the theory requires the rates of various transitions in the catalytic cycle of the motor. We follow previous studies (44, 57) to extract the kinetic rates in our model (Fig. 1*C*). We emphasize that the current analysis focuses only on the forward stepping cycle of kinesin. Although the cycle for the backward steps is certainly necessary to model the complete energetics of dimeric molecular motors, the mechanism of how kinesin takes backward steps is still under debate, which implies that there could be significant uncertainties

in the energetics in modeling the backward steps. Nevertheless, it is worth pointing out that as long as the probability of taking backward steps is small, which is certainly the case as long as the external load is below the stall force (58), the connection between information transfer and gating predicted by the theory should be valid. The two new high spatial and temporal experiments (59, 60) suggest that the backward stepping of kinesin is the process of recovering from the detachment on the polar track. Thus, the back steps for kinesins may not require any communication in terms of chemical reactions, that is, purely mechanical slide on MT. Fig. 1C focuses on the forward cycle of kinesin because here the gating and its behavior in forward steps of the motor is of interest. To minimize the effect of backward steps, we did not consider negative velocities (5 pN  $\lesssim F$ ) in the experimental force-velocity data (41) in order to extract the kinetic parameters needed to characterize the reaction cycle in Fig. 1C. The detailed description of the procedure to calculate the parameters and their values is provided in SI Appendix, section II.

Because our theory is based on thermodynamics, it is important to assess whether the model in Fig. 1C reflects the energetics in kinesin in the experiment (41). Specifically, the input energy needed to drive the catalytic cycle in the experiment ( $\Delta\mu_{ex}$ ) has to equal to the sum of dissipated heat (Q) and work done by kinesin (W) calculated using the network shown in Fig. 1C. In Fig. 2 A and B, we plot the rate for  $\Delta\mu_{ex}$  and  $\Delta\mu\equiv Q+W$ , obtained by multiplying each quantity by the steady-state current in the network using the parameters listed in SI Appendix, Table S1. The agreement between the calculations and experiment is excellent for both two sets of nucleotide concentrations. Thus, we conclude that the network used in the analysis describes the thermodynamics of energy consumption in kinesin accurately.

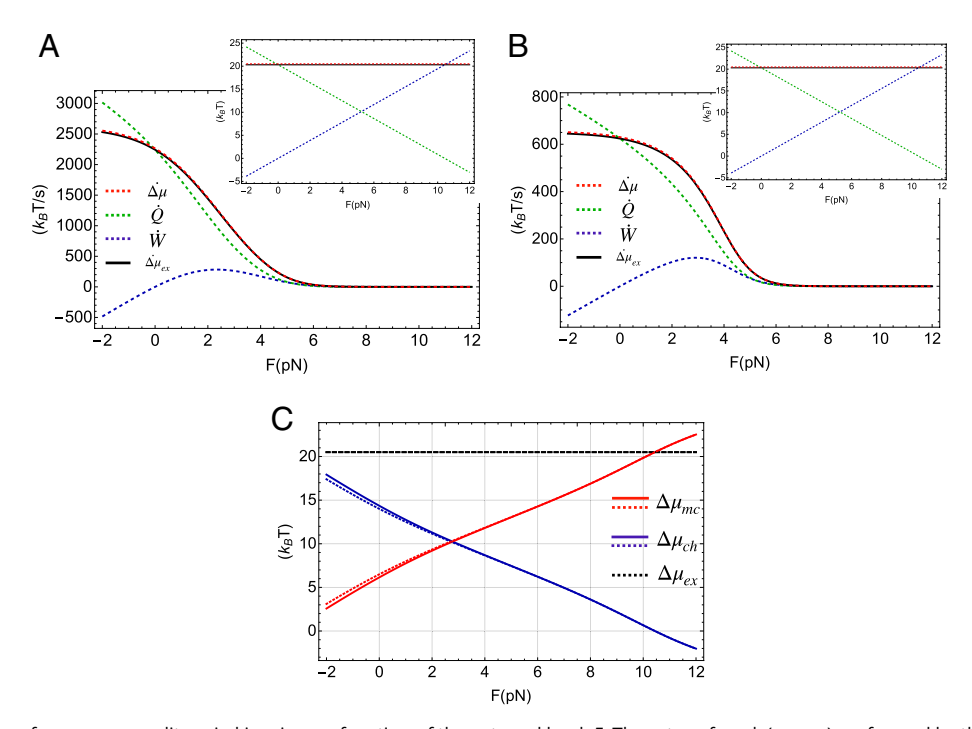


**Fig. 2.** (*A* and *B*) Rates of energy expenditure in kinesin as a function of the external load, *F*. The rates of work (power) performed by the motor and the rate of heat dissipation calculated from the kinetic network in Fig. 1*C* are denoted as  $\dot{W}$  and  $\dot{Q}$ , respectively. The sum of  $\dot{W}$  (blue dashed line) and  $\dot{Q}$  is  $\dot{\Delta}\mu$  (green dashed line). The rate of input energy in the single-molecule experiment (41) (black) is  $\dot{\Delta}\mu_{ex}$ . *Insets* show the corresponding bare quantities,  $\dot{W}$  (blue dashed line),  $\dot{Q}$  (green dashed line),  $\dot{Q}$  (red dashed line), and  $\dot{\Delta}\mu_{ex}$  (black solid line). (*A*) [T] = 1 mM, [D] = 0.1 mM, and [P<sub>i</sub>] = 1 mM. (*B*) [T] = 10 μM, [D] = 1 μM, and [P<sub>i</sub>] = 1 mM. Under both conditions,  $\dot{\Delta}\mu \approx \dot{\Delta}\mu_{ex}$ , which not only validates the theory but also shows that the extracted parameters for kinesin (*Sl Appendix*, Table S1) using different observables are reasonable. (*C*) Allocation of the input chemical energy for mechanical transition ( $\dot{\Delta}\mu_{mc}$ ) and chemical transitions ( $\dot{\Delta}\mu_{ch}$ ) as a function of *F*. The results are obtained theoretically for the kinesin network in Fig. 1C. The black dashed line shows the experimental value,  $\dot{\Delta}\mu_{ex}$ , which is the energy input. Solid lines are for [T] = 1 mM, [D] = 0.1 mM, [P<sub>i</sub>] = 1 mM, and dotted lines are for [T] = 10 μM, [D] = 1 μM, [P<sub>i</sub>] = 1 mM. The calculated sum,  $\dot{\Delta}\mu_{ch} + \dot{\Delta}\mu_{mc}$ , is equal to  $\dot{\Delta}\mu_{ex}$ .

Two different nucleotide concentrations [T] = 1 mM, [D] =0.1 mM, [P] = 1 mM and  $[T] = 10 \mu\text{M}$ ,  $[D] = 1 \mu\text{M}$ , [P] =1 mM were used in the experiments (41). Under both the conditions, the input energy ( $\Delta \mu_{ex} = 84.5 \text{ pN} \cdot \text{nm} \approx 20.5 \ k_B T$ ) is the same because [T]/([D][P]) is identical. The ideal stall load ( $F_{max}$ ) may be estimated using  $F_{max} = 20.5 (k_B T) \cdot 4.1$  $(\text{nm}\cdot\text{pN}/k_B\,T)/8(\text{nm})=10.5\,\text{pN},$  where 8 nm is the step size of kinesin. However, the measured stall load  $(F_s)$  for Kin-1 is in the range  $6\,\mathrm{pN} \lesssim F_s \lesssim 8\,\mathrm{pN}$  (61–63). The reason for this is that pathways, besides the forward steps, become relevant when F exceeds a critical value (discussed further below).

The mechanisms of stepping kinetics in motors are usually inferred by applying an external load to the cargo (Fig. 1A) in singlemolecule optical tweezer experiments. In order to extract the motor energetics from such experiments, one has to be cautious, because heat dissipation occurs in a multidimensional energy landscape, while experiments only report the dynamics along one experimentally accessible dimension, stepping direction, which is aligned with F. This is clear because a source of hidden dissipation, which cannot be accessed by observing only the steps, is the energy expended to drive the chemical transitions. Thus, only a portion of the input energy is used for mechanical stepping. We calculated  $\Delta\mu_{ch}$  and  $\Delta\mu_{mc}$  as a function of F (Fig.  $2\hat{C}$ ) in order to determine the allocation of the input energy  $(\Delta \mu_{ex})$ , at the two different nucleotide concentrations used in the experiment, for mechanical stepping ( $\Delta \mu_{mc}$ ) and chemical transitions ( $\Delta \mu_{ch}$ ). The values of  $\Delta \mu_{mc}$  and  $\Delta \mu_{ch}$  are almost identical under both the conditions, suggesting that the allocation does not depend on the nucleotide concentrations. From the plots in Fig. 2C, we find that  $\Delta \mu_{mc} \approx 9.2 \, k_B \, T$  and  $\Delta \mu_{ch} \approx 11.3 \, k_B \, T$  at F=2 pN, the value of resistive force used to estimate heat dissipation kinesin in the experiment (41). Thus, at most, 45% of the input energy is used to drive mechanical stepping at F = 2 pN. As F increases,

the energy needed to drive the mechanical step increases, which must come at the expense of a decrease in the  $\Delta\mu_{ch}$  for executing the chemical transitions. We note that the analysis by Pietzonka et al. (64) and Seifert (65) using the thermodynamics uncertainty relation also suggests similar efficiency at 2 pN. Although, theoretically, the entire input energy could be used for stepping at  $F = 10.5 \,\mathrm{pN}$  (Fig. 2C) only by maintaining the forward cycle at equilibrium, it cannot be realized at all, because CS transitions that cost energy have to occur for the motor to step forward. It also follows that the ideal stall force  $F_{max} = 10.5 \,\mathrm{pN}$ , which cannot be obtained in experiments because, at moderately high forces (F > 5 pN), backward steps start to be prominent.

We note that some kinetic networks, which successfully reproduce negative velocity for kinesin at large F, are based on a dual cycle network for the forward and backward cycles (44, 57). We analyze such a model in SI Appendix, section V. It turns out that the information flow stemming from the backward cycle results in a convex form of  $\Delta i$ ; initially,  $\Delta i$  decreases as  $\vec{F}$  increases, corresponding to the decrease in the information flow in the forward cycle. As F continues to increase,  $\Delta i$  increases because the information flow in the backward steps starts to become relevant. Nevertheless, if we separate the net information flow into the contributions from the forward and backward cycles,  $\Delta i$ in the forward cycle is qualitatively similar to the prediction in Fig. 3A. We emphasize that the free-energy transduction occurs in the two cycles independently. In other words, energy conservation  $(\Delta \mu = Q + W)$  holds in both cycles independently. Thus, we can consider energetics in the forward steps separately from backward steps, as discussed in this section.

The discrepancy between  $F_{\it max}$  and  $F_{\it s}$  is a consequence of the nonequilibrium nature of the stepping transition, which creates alternate stepping pathways that consume energy. The stall of kinesin is a consequence of the dynamic equilibrium between the

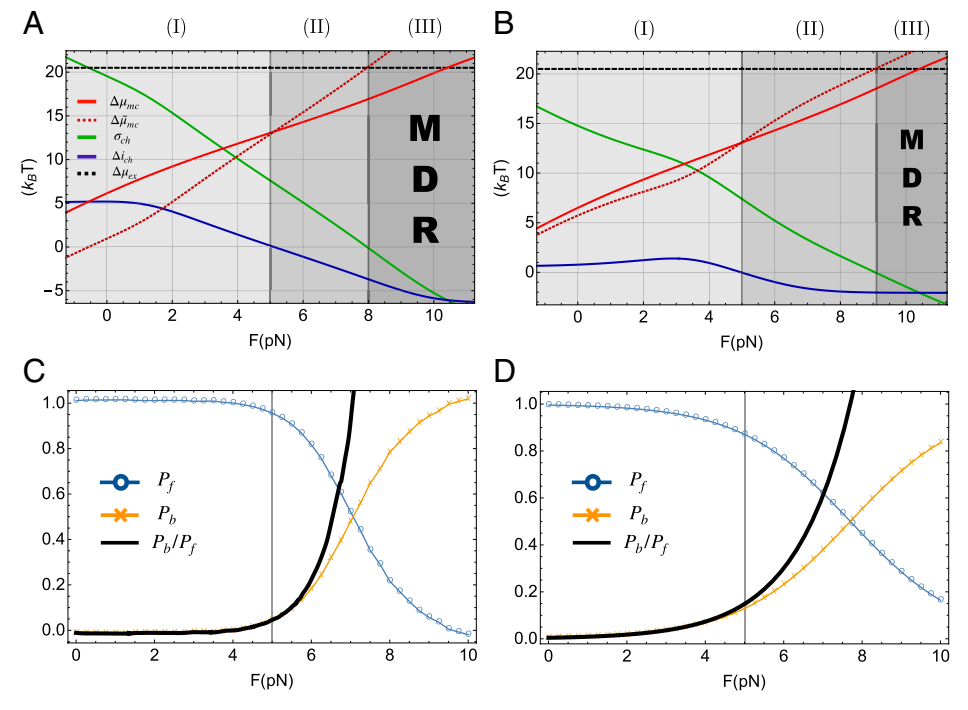


Fig. 3. Analysis of the experimental data using theory. (A and B) Contribution of each term in Eqs. 7. and 9;  $\Delta \mu_{mc}$  is the energy needed for driving the mechanical step,  $\sigma_{ch}$  is the apparent entropy production in the chemical transitions,  $\Delta i_{ch}$  is the change in the PMI during chemical transitions, and  $\Delta \mu_{ex} = 0$  $20.5 k_BT$  is the input chemical energy from the experiment (41). The apparent energy expended to drive the chemical transitions is  $\Delta \tilde{\mu}_{ch}$ . The gray colors and the corresponding numbers are the three regimes explained in the text. (A) [T] = 1 mM, [D] = 0.1 mM, and  $[P_i] = 1$  mM. (B) [T] = 10  $\mu$ M, [D] = 1  $\mu$ M, and  $[P_i]=1$  mM. In both A and B, the regime corresponding to  $\Delta\mu_{mc}$  exceeding  $\Delta\mu_{ex}$  is physically not allowed. (C) The probability for the forward step  $(P_f;$  blue), the backward step  $(P_b;$  yellow), and the fraction  $(P_b/P_f;$  black), calculated from ref. 44 (SI Appendix, section III). F=5 pN is highlighted by the gray line where  $\Delta i_{ch}=0$  . (D) Same as C except the stepping probabilities are calculated using a theory developed elsewhere (10).

cycles for forward and backward stepping. It is important to note that backward steps start to be prominent, typically at  $\approx$ 5 pN (44, 62) in kinesin, leading to the experimentally observed value of  $F_s$ that is considerably less than  $F_{max}$ . We discuss this discrepancy by computing  $\Delta i_{ch}$ , the quantification of the cooperativity.

Cooperative Information Flow Ceases as Backward Step Proba**bility Increases.** In Fig. 3, we plot the *F*-dependent information flow,  $\Delta i_{ch}$ , and the apparent entropy production  $\sigma_{ch}$  during the chemical transitions. The plot naturally divides itself into three regimes, depending on the signs of  $\Delta i_{ch}$  and  $\sigma_{ch}$ . In regime I,  $F \lesssim 5$  pN, where  $0 \leq \Delta i_{ch}$  and  $0 \leq \sigma_{ch}$ . In this force range, there is positive cooperativity between the TH and the MT bound LH, thus making the gating process effective, which, in turn, results in the motor walking processively on the MT.  $P_b$ , backward step probability, is small ( $P_b \leq 0.05$ ). In regime II, in the range 5pN  $\lesssim F \lesssim 8$  pN to 9 pN,  $\Delta i_{ch} \leq 0$  and  $0 \leq \sigma_{ch}$ . At F = 5pN,  $\Delta i_{ch}$  vanishes (Fig. 3 A and B). Not coincidentally,  $P_b$  starts to increase rather steeply at  $F \approx 5 \text{pN}$  (Fig. 3 C and D). Interestingly, the value of F at which  $\Delta i_{ch} = 0$  is independent of the nucleotide concentrations, as can be noted by comparing Fig. 3 A and B. The near independence of  $F_c$  on nucleotide concentration is dramatically illustrated in SI Appendix, Fig. S2. It shows that  $F_c$  changes by less than  $0.2\,\mathrm{pN}$  as ATP and ADP concentrations change by nearly three orders of magnitude. In regime III, in the force range 8 pN to 9 pN  $\lesssim F$ , both  $\Delta i_{ch} \leq 0$ and  $\sigma_{ch} \leq 0$ . Note that, at F > 10.5 pN, the direction of the stationary flow reverses, leading to the theoretical possibility of ATP synthesis with  $\Delta\mu_{mc}>\Delta\mu_{ex}$ . Although ATP synthesis with a slow rate for kinesin is possible (66), the backward step by ATP synthesis and release of products has not been observed. Hence, this regime is excluded in our analysis.

The results in Fig. 3 along with Eqs. 6-8 allow us to make the following observations. In regime I,  $\Delta i_{ch}$  is positive, which shows that gating is most effective. Interestingly, Hwang and Hyeon (44) have shown, using the thermodynamic uncertainty relation, that transport efficiency is optimized in this force range. In regime II, the information flow is less than optimal. This regime (≈5 pN) coincides with the initiation of backward stepping by kinesin, as shown in Fig. 3 C and D (further explained below). Thus, the loss of efficient communication between the motor heads  $(\Delta i_{ch} < 0)$  leads to kinesin taking backward steps (the LH could detach prematurely and goes toward the minus end of MT by hydrolyzing ATP). In regime III,  $\sigma_{ch}$  is negative, which we refer to as the MDR.

Fig. 3 C and D shows the probability of forward step  $(P_f)$ , backward step  $(P_b)$ , and the ratio  $(P_b/P_f)$  calculated in previous studies (10, 44) (SI Appendix, section III). The probabilities shown in Fig. 3C are from the six-state double-cycle model in ref. 45, and the probabilities in Fig. 3D are from the random walk model (10). In light of recent studies (59, 60), it is unclear whether either study, which account for backward steps for the purposes of fitting experimental data, is correct. Our unicycle model only considers the forward cycle. We remark that, because the two studies (10, 44) used kinetic models different from the current network model in Fig. 1*C*, the connection to our study is indirect. Nevertheless, the results in Fig. 3 C and D allow us to provide the physical meaning of  $F_c$  that emerges from the use of information theory for gating:  $\Delta i_{ch} = 0$  signifies the transition from positive cooperativity to negative cooperativity. It is gratifying that, despite significant differences between the kinetic models used in the previous studies (10, 44), it is clear that the effect of backward steps becomes prominent at  $F_c \approx 5 \, \mathrm{pN}.$  Furthermore, the loss of information flow at  $F_c$  is a robust feature.

It is possible to give an intuitive explanation for MDR by thermodynamic interpretation. Let us define  $\Delta \tilde{\mu}_{ch}$  and  $\Delta \tilde{\mu}_{mc}$  as

$$\Delta \tilde{\mu}_{ch} = \sigma_{ch}, \qquad [9]$$

$$\Delta \tilde{\mu}_{mc} = \Delta \mu - \sigma_{ch}.$$
 [10]

The above two equations, Eqs. 9 and 10, should be compared with Eqs. 6 and 7, respectively;  $\Delta \tilde{\mu}_{ch}$  ( $\Delta \tilde{\mu}_{mc}$ ) is the apparent energy expended for chemical (mechanical) transition if we have no knowledge of interhead communication  $\Delta i_{ch}$ . We can imagine such a scenario for dimeric motors if one can only access the chemical transitions in one head. If we construct the network of CSs for the dimeric motor by simply integrating the observation from a single motor head, it would lead to the apparent energy transduction given in Eqs. 9 and 10. In Fig. 3,  $\Delta \tilde{\mu}_{mc}$  reaches and exceeds  $\Delta \mu_{ex}$  in MDR. This superficially suggests that the motor could use more energy to execute the mechanical transition than the input energy  $\Delta \mu_{ex}$ . Thus, without accounting for the interhead communication,  $\Delta i_{ch}$ , we would obtain inconsistent energetics in motors. In this interpretation, the bound head may be thought of as the Maxwell demon in the sense that it has information about the trailing or diffusing head. This could be the thermodynamic interpretation of the Maxwell demon in dimeric motors.

## Myosin V

In order to establish that gating, controlled by information flow between the motor heads, is applicable to other motors, we next considered the chemomechanical network for myosin V (Fig. 4A), a motor that also walks by a hand-over-hand mechanism on Factin by taking 36-nm steps. The chemomechanical model with three cycles was proposed by Bierbaum and Lipowsky (67). The energetic cost, precision, and efficiency associated with the network were investigated recently by Hwang and Hyeon (44). The cycle,  $\mathcal{F}$ , is the one that requires chemical coordination leading to the mechanical step. The cycle  $\epsilon$  is the futile cycle that consumes energy but does not lead to a mechanical step. The cycle  ${\cal M}$  is spontaneous stepping without chemical reactions.

Our focus is on the information flow in the cycle  ${\cal F}$  in which mechanical transition requires the coordination of the CSs between the two motor heads. Because experimental data for the concentration of ADP and phosphate for myosin V are not available, we set  $[D] = 70 \mu M$  and  $[P_i] = 1 \text{ mM}$ , which is appropriate for the in vivo condition (44). We analyzed the high ATP concentration [T] = 1 mM and low ATP concentration [T] = 1  $\mu$ M. The nucleotide concentrations [T] = 1mM [D] = 70  $\mu$ M  $[P_i] = 1$  mM give chemical energy input  $\Delta \mu \approx 22.7 \ k_B T$ , and [T] = 1  $\mu$ M [D] = 70  $\mu$ M [P<sub>i</sub>] = 1 mM gives chemical energy input  $\Delta\mu \approx 15.8~(k_B\,T)$ . These values were calculated using the relation  $\mu = k_B T \ln K_{eq}[T]/([D][P])$ , where  $K_{eq} =$  $4.9 \cdot 10^{11} \mu \mathrm{M}$  is the corresponding equilibrium constant (68). The expected ideal stall load is  $F_{max} \approx 2.6$  pN and  $F_{max} \approx$ 1.8 pN for [T] = 1 mM [D] = 70  $\mu$ M [P<sub>i</sub>] = 1 mM and [T] =  $1 \mu M [D] = 70 \mu M [P_i] = 1 mM$ , respectively. Note that the two set nucleotide concentrations yield different amounts of input

Just as in Kin-1, there are three regimes. In regime I,  $\Delta i_{ch} \geq 0$ and  $\sigma_{ch} \geq 0$  if  $F \lesssim 1$  pN; in regime II,  $\Delta i_{ch} \leq 0$  and  $\sigma_{ch} \geq 0$  for 1pN  $\lesssim F \lesssim 1.4$  pN to 1.8 pN; and, in regime III,  $\Delta i_{ch} \leq 0$  and  $\sigma_{ch} \leq 0$  for  $1.4\,\mathrm{pN}$  to  $1.8\,\mathrm{pN} \lesssim F$ , depending on the nucleotide concentrations. In regime I (Fig. 4 C and D),  $\Delta i_{ch}$  is positive, suggesting that communication between the motor heads is efficient, resulting in the forward stepping of the motor with the

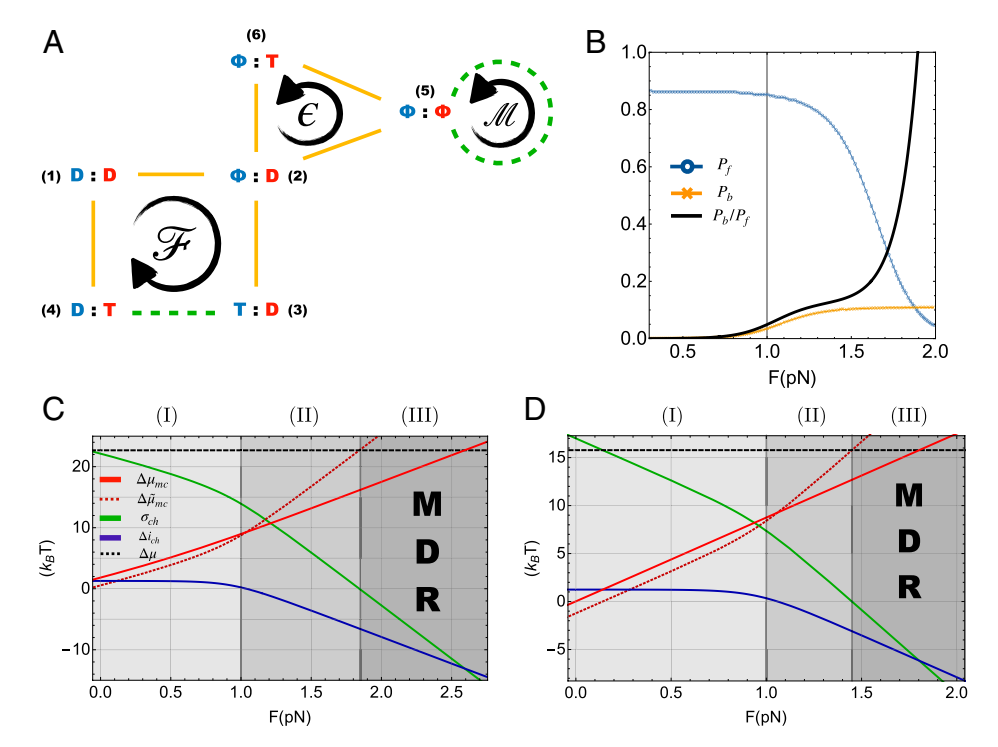


Fig. 4. (A) Chemomechanical cycle for myosin V. The diagram shows three cycles,  $\mathcal{F}$ ,  $\epsilon$ , and  $\mathcal{M}$ .  $\mathcal{F}$  is associated with stepping utilizing chemical energy by ATP hydrolysis;  $\epsilon$  is a futile cycle in which ATP is consumed but the motor does not step;  $\mathcal M$  describes mechanical stepping without ATP hydrolysis. In yellow are the chemical transitions, and the transitions in dashed green are mechanical transitions. Blue and red colors describe the CSs in the two heads of the motor. The cycle is adopted from refs. 44 and 67. (B) The probability for the forward step  $(P_f)$ , the backward step  $(P_b)$ , and the fraction  $(P_b/P_f)$ , digitized from ref. 25. The gray line highlights  $F \approx 1$  pN where  $\Delta i_{ch}$  becomes negative. Note that, at all values of F,  $P_f + P_b \neq 1$ , because there are pathways associated with stomping of the LH and TH (25). (C and D) Plots for the terms in Eqs. 7 and 9. for myosin V.  $\Delta \mu_{mc}$  is the chemical energy allocated to the mechanical stepping,  $\sigma_{ch}$  is the apparent entropy production during chemical transitions,  $\Delta i_{ch}$  is the change of PMI during chemical transitions, and  $\Delta \mu$  is the chemical energy input at given nucleotide concentrations.  $\Delta ilde{\mu}_{ch}$  is the apparent energy spent for chemical transitions. Gray regions and the corresponding numbers are the three regimes explained in the text. [T] = 1 mM, [D] = 70  $\mu$ M, [P] = 1 mM and [T] = 1  $\mu$ M, [D] = 70  $\mu$ M, [P] = 1 mM for C and D, respectively. The regimes in which  $\Delta \mu_{mc}$  exceeding  $\Delta \mu_{ex}$  (ATP synthesis) cannot occur. Regime III would be prevented, in practice, by enhanced probabilities of other cycles (for instance,  $\epsilon$ and  $\mathcal{M}$ ).

probability of stepping backward being negligible. In regime II, the motor loses efficient interhead communication ( $\Delta i_{ch} \leq 0$ ), and the amount of available energy from the gating for mechanical transition diminishes, which is indicated by the negative  $\Delta i_{ch}$ . This may trigger the increased propensity for the myosin V to step backward. A previous theoretical study (25) showed that backward steps start to be relevant at  $F \approx 1$  pN (Fig. 4B), which is the value of force at which  $\Delta i_{ch} = 0$ . The concentrations of ADP and Pi are typically not controlled explicitly in experiments, which may lead to variations in  $\Delta \mu_{ex}$ . Thus, estimates of the energetics,  $F_s$  for instance, in various experiments and physiological concentrations for myosin V from different experiments may not be comparable to the results in Fig. 4 C and D. Nevertheless, the resistive load that signals the transition from regime II to III is in the range of the experimentally observed stall force  $[1.6\,\mathrm{pN} \lesssim F_s \lesssim 2.0\,\mathrm{pN}]$ (69-75)].

## **Discussion and Conclusion**

The language and interpretation from information theory are extended to illustrate the meaning of gating, an elusive but important concept, in molecular motors. In the framework developed here, gating is viewed as information flow between the two heads of the motor. Communication between the motor heads, which is a qualitative description of gating, has been invoked as the basis for processivity in molecular motors. Our theory quantifies the gating phenomenon in terms of parameters that characterize the steps in the catalytic cycle of dimeric molecular motors. The theory is potentially applicable to a broad class of biological machines.

We first derived an equality relating the change in PMI to heat dissipation along a transition in a driven kinetic network. By using our theory, we quantified gating in Kin-1 and myosin V. The two most important findings are the following. First, we showed that gating is cooperative at resistive forces less than a critical value,  $F_c$ , which means that communication between the two heads is effective. As a consequence, the chemical transitions results in the TH detaching with much greater probability than the LH. In this case, the probability that the motor takes a forward step far exceeds the probability of backward steps.

Second, as the magnitude of the force increases, there is a loss in gating efficiency, and information  $\Delta i_{ch}$  becomes negative. The transition between low-force positive cooperative interaction between the motor heads and loss of interhead communication, due to negative cooperativity, occurs at  $F_c$  where  $\Delta i_{ch} = 0$ . At  $F_c$ , there is a lack of correlation (or communication) between the two heads. Surprisingly, for both the motors, the values of  $F_c$ , which is independent of the input energy, coincide when the probability for backward transition starts to increase.

Our findings show that, despite the significant differences in the chemical cycle and the architecture of Kin-1 and myosin V, we obtain similar results with regard to the force-dependent information flow, and hence gating. This is not a coincidence; this class of motors has evolved to work efficiently at forces less than  $F_c$ . Efficient gating could be the universal working principle in dimeric molecular motors, which means that  $F < F_c$  under in vivo conditions.

Our main result for kinesin, using the cycle sketched in Fig. 1 C, does not consider the information flow associated with backward steps. Because the mechanism of backward steps is still under debate (59, 60), a quantitative measure of information flow in the net cycle for kinesin (forward plus backward steps) cannot be provided at present. The information flow at high external loads could depend on the CSs that the motor explores during the backward cycle. When the mechanism of backward steps is made clear, the theory can be extended to model the entire cycle. However, we believe that one of our key results concerning the loss of coordination between the motor heads at forces less than the stall force but greater than  $F_c$  is likely to be robust.

We are now in a position to provide an interpretation of positive information flow, which results in kinesin taking multiple steps toward the plus end of the MT without detaching. The coordination between motors (Fig. 1C) may be quantified using

$$\Delta i = k_B \left( \ln \frac{p(X = T, Y = D)}{p_X(T)p_Y(D)} - \ln \frac{p(X = D, Y = T)}{p_X(D)p_Y(T)} \right).$$
[11]

We identified X is the LH and Y is the TH. For this value to be large and positive, which implies effective communication, the CSs of the two heads must be more correlated in state 5 (before the mechanical step) than in state 1 (after the step). In other words,  $(p(X = T, Y = D)/p_X(T)p_Y(D)) >$  $(p(X = D, Y = T)/p_X(D)p_Y(T))$ . The reason for this is intuitive: Once the CS before the mechanical step is reached, it does not behoove the motor to leave that state, and thus it is beneficial to have strong correlation between the CSs of the two heads. In contrast, after the mechanical step is completed (state 1), the CS of the two heads should be loosely correlated, in order to immediately leave the landing state, which is amenable to revert the step. We note that this is realized in molecular motors: Upon completing a mechanical step by binding to the track, kinesin and myosin release ADP and phosphate, respectively, which consolidates the two-head-bound state, which, in the framework of this paper, means that  $p(X = D, Y = T)/p_X(D)p_Y(T)$  should be small.

The asymmetry between the CSs, that arises in our formulation, could be related to the notion of "kinetic asymmetry" (76-78) for the gating in motors. From Eq. **8**, we realize that  $\mathrm{e}^{(\Delta \mu_{mc} - W)/k_B}$ creates asymmetry in the steps. When  $e^{(\Delta \mu_{mc} - W)/k_B} > 1$ , then the motor steps forward, and, when  $\mathrm{e}^{(\Delta\mu_{mc}-W)/k_B}<1$ , the motor takes reverse steps. One can show that  $\Delta \mu_{mc} - W = \rho$ increases with  $\Delta i_{ch}$ . This indicates that the positive  $\Delta i_{ch}$  indeed amplifies the asymmetry in the steps that the motor takes. Quantifying the asymmetry in the selection of the forward cycle over the backward cycle requires understanding the mechanism of the backward steps in motors. Future experimental and theoretical studies would elucidate the connection of our study to the kinetic asymmetry (76–78).

Our analysis explains the reason for the apparent inefficiency of kinesin (41). For mechanical stepping to happen ((5) $\rightarrow$  (1) in Fig. 1C), kinesin has to first undergo chemical transitions ((1) $\rightarrow$ (5) in Fig. 1C). If the motor were to take a forward step, a certain amount of energy has to be expended to complete the chemical transitions at all values of F. At forces exceeding  $F_c \approx 5 \,\mathrm{pN}$ , there is a breakdown in interhead communication. As a result of loss of communication between the two heads and the increase in the mechanical energy to complete a step, other pathways (in particular, backward steps) become prominent. Although an experiment similar to the one for kinesin (41) has not been performed for myosin V, our prediction is that the results would be similar (myosin V would be most efficient if  $F \leq F_c \approx 1 \text{ pN}$ ).

From a structural perspective, information flow between the heads must be linked to action at a distance expressed in terms

of allostery (13). In kinesin, that walks on MT, the two heads are about 8 nm apart, whereas the distance between the motor heads in the F-actin bound myosin V is about 36 nm. How  $\Delta i_{ch}$ , the information flow, is linked to the structural changes in the motor driven by binding and hydrolysis of ATP followed by ADP release is unclear. The molecular link needs to be established before the design principles in naturally occurring motors can be fully understood.

#### Methods

**Information Flow on CS Transitions.** Let X(Y) undergo  $n_X$   $(n_Y)$  transitions along a specific path. The difference in the PMI between the initial and final state associated with the path,  $\Delta i_{i}$  can be calculated as  $\Delta i_{\chi} + \Delta i_{\chi}$ , where

$$\Delta i_{X} = \sum_{i=0}^{n_{X}-1} [i(x_{i+1}, y_{i}) - i(x_{i}, y_{i})]$$

$$= k_{B} \ln \prod_{i=0}^{n_{X}-1} \frac{\rho(y_{i}|x_{i+1})}{\rho(y_{i}|x_{i})},$$
[12]

where  $p(y_i|x_i) = p(x_i, y_i)/p_X(x_i)$  is a conditional probability. A similar expression holds for  $\Delta i_{\gamma}$ .

The bipartite property allows us to count the transitions for X and Y separately. Thus,  $(x_i, y_i)$  means the state of X and Y before the (i + 1)th transition for X, and, similarly,  $(x_i, y_i)$  for Y (Fig. 1B). The change in PMI along a path (for example,  $(1) \rightarrow (2)$  transition in Fig. 1*C*),  $\Delta i$ , is given by

$$\Delta i = k_B \ln \prod_{i=0}^{n_X-1} \frac{p(y_i|x_{i+1})}{p(y_i|x_i)} \prod_{j=0}^{n_Y-1} \frac{p(x_j|y_{j+1})}{p(x_j|y_j)}.$$
 [13]

**Entropy Production and Information Flow.** Entropy production,  $\rho$ , along a path in steady state can be decomposed as (26)

$$\rho = 0 + \Delta s_{XY}, \tag{14}$$

where

$$Q = k_B \ln \prod_{i=0}^{n-1} \frac{w_{x_i x_{i+1}}^{y_i y_{i+1}}}{w_{x_i x_{i+1} x_i}^{y_{i+1} y_i}}$$
 [15]

is the dissipated heat, and

$$\Delta s_{XY} = k_B \ln \prod_{i=0}^{n-1} \frac{\rho(x_i, y_i)}{\rho(x_{i+1}, y_{i+1})}$$
 [16]

is the change of the entropy for the system. In Eq. 15,  $w_{x_ix_{i+1}}^{y_iy_{i+1}}$  is the transition rate from state  $(x_i, y_i)$  to  $(x_{i+1}, y_{i+1})$ . We do not explicitly consider changes in the entropy of the motor protein due to conformational changes that invariably occur during the catalytic cycle. Although we could include it explicitly, this is not necessary, because heat dissipation together with the changes in the internal entropy could be lumped together (26). We avoid this unneeded complication because our theory is valid irrespective of the changes in internal conformational

Entropy production is always positive along the direction of stationary flow because  $p(x_i, y_i)w_{x_ix_{i+1}}^{y_iy_{i+1}} - p(x_{i+1}, y_{i+1})w_{x_{i+1}x_i}^{y_{i+1}y_i} > 0$  for all *i*. For a bipartite graph,  $\rho$  can be decomposed as

$$\rho = \rho_X + \rho_Y = (Q_X + \Delta s_{XY}^X) + (Q_Y + \Delta s_{XY}^Y),$$
 [17]

where

$$Q_{X} = k_{B} \ln \prod_{i=0}^{n_{X}-1} \frac{W_{x_{i}x_{i+1}}^{y_{i}}}{W_{x_{i+1}x_{i}}^{y_{i}}}; \Delta s_{XY}^{X} = k_{B} \ln \prod_{i=0}^{n_{X}-1} \frac{p(x_{i}, y_{i})}{p(x_{i+1}, y_{i})};$$

$$Q_{Y} = k_{B} \ln \prod_{i=0}^{n_{Y}-1} \frac{W_{x_{i}}^{y_{i}y_{i+1}}}{W_{x_{i}}^{y_{i}+1}y_{i}}; \Delta s_{XY}^{Y} = k_{B} \ln \prod_{i=0}^{n_{Y}-1} \frac{p(x_{i}, y_{i})}{p(x_{i}, y_{j+1})}.$$
[18]

The transition rate for  $(x_i, y_i) \rightarrow (x_{i+1}, y_i)$  (and  $(x_i, y_i) \rightarrow (x_i, y_{i+1})$ ) is denoted as  $w_{x_ix_{i+1}}^{y_i}$  ( $w_{x_i}^{y_iy_{i+1}}$ ). We can show that the equalities,  $\Delta s_X = \Delta s_{XY}^X + \Delta i_X$ and  $\Delta s_Y = \Delta s_{XY}^Y + \Delta i_Y$ , hold, where  $\Delta s_X = k_B \ln \prod_{i=0}^{n_X-1} (p_X(x_i)/p_X(x_{i+1}))$ and  $\Delta s_Y = k_B \ln \prod_{i=0}^{n_Y-1} (p_Y(y_i)/p_Y(y_{i+1}))$ . Using these relations, we obtain,

$$\rho_{X(Y)} = \sigma_{X(Y)} - \Delta i_{X(Y)}.$$
 [19]

In Eq. 19, we defined the apparent entropy production from X and Y as  $\sigma_X \equiv Q_X + \Delta s_X$  and  $\sigma_Y \equiv Q_Y + \Delta s_Y$ , respectively. By summing the terms in Eq. **19** for *X* and *Y*, we obtain Eq. **3** by defining  $\rho \equiv \rho_X + \rho_Y$  and  $\sigma \equiv \sigma_X + \sigma_Y$ .

**Mechanochemistry and Information.** We write the probability in state (i) as  $p_i$ . Namely, we use the notation  $p(X = D, Y = T) = p_1, p(X = \Phi, Y = T) = p_2$ and so forth. We denote the rate of transition from state (i) to state (j) as  $w_{ij}$ .

We can write the input chemical energy ( $\Delta\mu$ ) using the microscopic transition rates as

$$\Delta \mu = k_B \ln \frac{w_{12} w_{23} w_{34} w_{45} w_{51}}{w_{21} w_{32} w_{43} w_{54} w_{15}} + W,$$
 [20]

where W is the mechanical work done by the motor. Eq. 20 states that the affinity (driving force),  $k_B \ln(w_{12}w_{23}w_{34}w_{45}w_{51}/w_{21}w_{32}w_{43}w_{54}w_{15})$ , is obtained from the sum of free energy supplied by the chemical reaction ( $\Delta \mu$ ) and the work done to the motor (-W). For  $\Pi_{ch}$  where only chemical reactions matter, the affinity may be supplied from the chemical energy ( $\Delta\mu_{ch}$ ) and the change of internal energy  $(-k_B \ln \frac{\rho_1}{\rho_5})$ . Thus, we define

$$\Delta\mu_{ch} = k_B \ln \frac{w_{12}w_{23}w_{34}w_{45}}{w_{21}w_{32}w_{43}w_{54}} + k_B \ln \frac{\rho_1}{\rho_5}.$$
 [21]

- R. D. Vale, R. A. Milligan, The way things move: Looking under the hood of molecular motor proteins. Science 288, 88-95 (2000).
- R. D. Vale, The molecular motor toolbox for intracellular transport. Cell 112, 467-480 (2003).
- R. lino, K. Kinbara, Z. Bryant, Introduction: Molecular motors. Chem. Rev. 120, 1-4 (2020).
- C. L. Asbury, A. N. Fehr, S. M. Block, Kinesin moves by an asymmetric hand-over-hand mechanism. Science 302, 2130-2134 (2003).
- A. Yildiz et al., Myosin V walks hand-over-hand: Single fluorophore imaging with 1.5-nm localization. Science 300, 2061-2065 (2003).
- A. Yildiz, M. Tomishige, R. D. Vale, P. R. Selvin, Kinesin walks hand-over-hand. Science 303, 676-678
- Y. Z. Ma, E. W. Taylor, Interacting head mechanism of microtubule-kinesin ATPase. J. Biol. Chem. 272,
- M. Y. Dogan, S. Can, F. B. Cleary, V. Purde, A. Yildiz, Kinesin's front head is gated by the backward orientation of its neck linker. Cell Rep. 10, 1967-1973 (2015).
- H. Isojima, R. Iino, Y. Niitani, H. Noji, M. Tomishige, Direct observation of intermediate states during the stepping motion of kinesin-1. Nat. Chem. Biol. 12, 290-297 (2016).
- R. Takaki, M. L. Mugnai, Y. Goldtzvik, D. Thirumalai, How kinesin waits for ATP affects the nucleotide and load dependence of the stepping kinetics. Proc. Natl. Acad. Sci. U.S.A. 116, 23091-23099 (2019).
- 11. T. Sakamoto, M. R. Webb, E. Forgacs, H. D. White, J. R. Sellers, Direct observation of the mechanochemical coupling in myosin Va during processive movement. Nature 455, 128-132 (2008).
- 12. N. Kodera, D. Yamamoto, R. Ishikawa, T. Ando, Video imaging of walking myosin V by high-speed atomic force microscopy. Nature 468, 72-76 (2010).
- D. Thirumalai, C. Hyeon, P. I. Zhuravlev, G. H. Lorimer, Symmetry, rigidity, and allosteric signaling. From monomeric proteins to molecular machines. Chem. Rev. 119, 6788-6821 (2019).
- W. O. Hancock, J. Howard, Kinesin's processivity results from mechanical and chemical coordination between the ATP hydrolysis cycles of the two motor domains. Proc. Natl. Acad. Sci. U.S.A. 96, 13147-13152 (1999).
- A. Yildiz, M. Tomishige, A. Gennerich, R. D. Vale, Intramolecular strain coordinates kinesin stepping behavior along microtubules. Cell 134, 1030-1041 (2008).
- C. Hyeon, J. N. Onuchic, Internal strain regulates the nucleotide binding site of the kinesin leading head. Proc. Natl. Acad. Sci. U.S.A. 104, 2175-2180 (2007).
- S. Shastry, W. O. Hancock, Neck linker length determines the degree of processivity in kinesin-1 and kinesin-2 motors. Curr. Biol. 20, 939-943 (2010).
- Z. Zhang, D. Thirumalai, Dissecting the kinematics of the kinesin step. Structure 20, 628-640 (2012).
- B. E. Clancy, W. M. Behnke-Parks, J. O. Andreasson, S. S. Rosenfeld, S. M. Block, A universal pathway for kinesin stepping. Nat. Struct. Mol. Biol. 18, 1020-1027 (2011).
- J. O. Andreasson et al., Examining kinesin processivity within a general gating framework. eLife 4
- 21. B. Milic, J. O. Andreasson, W. O. Hancock, S. M. Block, Kinesin processivity is gated by phosphate release. Proc. Natl. Acad. Sci. U.S.A. 111, 14136-14140 (2014).
- S. S. Rosenfeld, P. M. Fordyce, G. M. Jefferson, P. H. King, S. M. Block, Stepping and stretching. How kinesin uses internal strain to walk processively. J. Biol. Chem. 278, 18550–18556 (2003).
- E. Toprak, A. Yildiz, M. T. Hoffman, S. S. Rosenfeld, P. R. Selvin, Why kinesin is so processive. Proc. Natl. Acad. Sci. U.S.A. 106, 12717-12722 (2009).

For  $\Pi_{mc}$ , we include the contribution from the mechanical work,

$$\Delta\mu_{mc} = k_B \ln \frac{w_{51}}{w_{15}} + k_B \ln \frac{\rho_5}{\rho_1} + W.$$
 [22]

The definition of Eqs. 21 and 22 satisfying Eq. 5 separates energy consumption in the chemomechanical cycle into chemical and mechanical expenses. This is explicitly demonstrated in Fig. 2for kinesin, in the following section.

For  $\Pi_{mc}$ , we can rewrite Eq. **22** in the following form:

$$\Delta\mu_{mc} - W = \rho_{mc}$$
, [23]

where  $ho_{\it mc}=k_{\it B}\ln{\frac{w_{\rm 51}\rho_{\rm 5}}{w_{\rm 15}\rho_{\rm 1}}}$  is the entropy production in  $\Pi_{\it mc}$ .  $\rho_{\it mc}$  quantifies the nonequilibrium nature of the motor stepping; in other words,  $\rho_{\it mc}=0$  at equilibrium. rium, which is a consequence of the detailed balance condition in Fig. 1C. Using  ${
m e}^{(\Delta\mu_{mc}-W)/k_B}=(p_5w_{51})/(p_1w_{15})$  from Eq.  ${f 23}$  and the flux associated with the mechanical step,  $J_{mc} = p_5 w_{51} - p_1 w_{15}$ , we obtain Eq. **8**.

Data, Materials, and Software Availability. All study data are included in the article and/or SI Appendix. The file used to generate the figures has been deposited in GitHub (https://github.com/kibidanngo/Information-flow-PNAS) (79).

**ACKNOWLEDGMENTS.** We are grateful to Jordon Horowitz for several useful comments on an earlier version of the manuscript. This work is part of the doctoral thesis of R.T. Most of the work was completed while R.T. and M.L.M. were associated with the University of Texas at Austin. We are grateful to the NSF (Grant CHE 19-00093), and Welch Foundation Grant F-0019 through the Collie-Welch chair, for supporting this work.

Author affiliations: <sup>a</sup>Department of physics, The University of Texas at Austin, Austin, TX; <sup>b</sup>Department of chemistry, The University of Texas at Austin, Austin, TX; and <sup>c</sup>Department of chemistry and department of physics, The University of Texas at Austin, Austin, TX

- 24. Y. Miyazono, M. Hayashi, P. Karagiannis, Y. Harada, H. Tadakuma, Strain through the neck linker ensures processive runs: A DNA-kinesin hybrid nanomachine study. EMBO J. 29, 93-106 (2010).
- M. Hinczewski, R. Tehver, D. Thirumalai, Design principles governing the motility of myosin V. Proc. Natl. Acad. Sci. U.S.A. 110, E4059-E4068 (2013).
- U. Seifert, Stochastic thermodynamics, fluctuation theorems and molecular machines. Rep. Prog. Phys. 75, 126001 (2012).
- K. Sekimoto, Stochastic Energetics (Lecture Notes in Physics, Springer, 2010), 799
- D. Kondepudi, I. Prigogine, Modern Thermodynamics: From Heat Engines to Dissipative Structures (John Wiley, 2014).
- M. L. Mugnai, C. Hyeon, M. Hinczewski, D. Thirumalai, Theoretical perspectives on biological machines. Rev. Mod. Phys. 92, 025001 (2020).
- T. Sagawa, M. Ueda, Second law of thermodynamics with discrete quantum feedback control. Phys. Rev. Lett. 100, 080403 (2008).
- T. Sagawa, M. Ueda, Minimal energy cost for thermodynamic information processing: Measurement and information erasure. Phys. Rev. Lett. 102, 250602 (2009).
- J. M. Parrondo, J. M. Horowitz, T. Sagawa, Thermodynamics of information. Nat. Phys. 11, 131 (2015).
- S. Toyabe, T. Sagawa, M. Ueda, E. Muneyuki, M. Sano, Experimental demonstration of information-to-energy conversion and validation of the generalized Jarzynski equality. Nat. Phys. 6, 988-992 (2010).
- S. Ito, T. Sagawa, Maxwell's demon in biochemical signal transduction with feedback loop. *Nat.* Commun. 6, 7498 (2015).
- P. Sartori, L. Granger, C. F. Lee, J. M. Horowitz, Thermodynamic costs of information processing in sensory adaptation. PLOS Comput. Biol. 10, e1003974 (2014).
- J. M. Horowitz, T. Sagawa, J. M. Parrondo, Imitating chemical motors with optimal information motors Phys. Rev. Lett. 111, 010602 (2013).
- E. Penocchio, F. Avanzini, M. Esposito, Information thermodynamics for deterministic chemical reaction networks. J. Chem. Phys. 157, 034110 (2022).
- D. Loutchko, M. Eisbach, A. S. Mikhailov, Stochastic thermodynamics of a chemical nanomachine: The channeling enzyme tryptophan synthase. J. Chem. Phys. 146, 025101 (2017).
- E. Lathouwers, D. A. Sivak, Internal energy and information flows mediate input and output power in bipartite molecular machines. Phys. Rev. E 105, 024136 (2022).
- S. Amano et al., Insights from an information thermodynamics analysis of a synthetic molecular motor. Nat. Chem. 14, 530-537 (2022).
- T. Ariga, M. Tomishige, D. Mizuno, Nonequilibrium energetics of molecular motor kinesin. Phys. Rev. Lett. 121, 218101 (2018).
- T. Harada, S. Sasa, Equality connecting energy dissipation with a violation of the fluctuation-response relation. Phys. Rev. Lett. 95, 130602 (2005).
- T. Harada, S. Sasa, Energy dissipation and violation of the fluctuation-response relation in nonequilibrium Langevin systems. Phys. Rev. E Stat. Nonlin. Soft Matter Phys. 73, 026131 (2006).
- W. Hwang, C. Hyeon, Energetic costs, precision, and transport efficiency of molecular motors. J. Phys. Chem. Lett. 9, 513-520 (2018)
- $W.\ Hwang,\ C.\ Hyeon,\ Quantifying\ the\ heat\ dissipation\ from\ a\ molecular\ motor's\ transport\ properties$ in nonequilibrium steady states. J. Phys. Chem. Lett. 8, 250-256 (2017).

- 46. H. Ge, H. Qian, Physical origins of entropy production, free energy dissipation, and their mathematical representations. Phys. Rev. E Stat. Nonlin. Soft Matter Phys. 81, 051133 (2010).
- S. Liepelt, R. Lipowsky, Steady-state balance conditions for molecular motor cycles and stochastic nonequilibrium processes. Europhys. Lett. 77, 50002 (2007).
- M. L. Mugnai, M. A. Caporizzo, Y. E. Goldman, D. Thirumalai, Processivity and velocity for motors stepping on periodic tracks. Biophys. J. 118, 1537-1551 (2020).
- J. M. Horowitz, M. Esposito, Thermodynamics with continuous information flow. Phys. Rev. X 4, 031015 (2014).
- $D.\ Hartich, A.\ C.\ Barato,\ U.\ Seifert,\ Stochastic\ thermodynamics\ of\ bipartite\ systems:\ Transfer\ entropy$ inequalities and a Maxwell's demon interpretation. J. State. Mech. Theory Exp. 2014, P02016 (2014).
- C. Cafaro, S. A. Ali, A. Giffin, Thermodynamic aspects of information transfer in complex dynamical systems. Phys. Rev. E 93, 022114 (2016).
- S. Ito, T. Sagawa, Information thermodynamics on causal networks. Phys. Rev. Lett. 111, 180603 (2013).
- 53. M. Esposito, G. Schaller, Stochastic thermodynamics for "Maxwell demon" feedbacks. Europhys. Lett.
- T. Sagawa, M. Ueda, Role of mutual information in entropy production under information exchanges. New J. Phys. 15, 125012 (2013).
- X. J. Zhang, H. Qian, M. Qian, Stochastic theory of nonequilibrium steady states and its applications. part I. Phys. Rep. 510, 1-86 (2012).
- R. Lipowsky, S. Liepelt, A. Valleriani, Energy conversion by molecular motors coupled to nucleotide hydrolysis. J. Stat. Phys. 135, 951-975 (2009).
- 57. S. Liepelt, R. Lipowsky, Kinesin's network of chemomechanical motor cycles. Phys. Rev. Lett. 98, 258102 (2007).
- Y. Taniguchi, T. Yanagida, The forward and backward stepping processes of kinesin are gated by ATP binding. Biophysics (Nagoya-Shi) 4, 11-18 (2008).
- S. Sudhakar et al., Germanium nanospheres for ultraresolution picotensiometry of kinesin motors. Science 371, eabd9944 (2021).
- A. Toleikis, N. J. Carter, R. A. Cross, Backstepping mechanism of kinesin-1. Biophys. J. 119, 1984-1994 (2020).
- 61. K. Svoboda, S. M. Block, Force and velocity measured for single kinesin molecules. Cell 77, 773-784
- 62. K. Visscher, M. J. Schnitzer, S. M. Block, Single kinesin molecules studied with a molecular force clamp. Nature 400, 184-189 (1999).

- 63. S. M. Block, C. L. Asbury, J. W. Shaevitz, M. J. Lang, Probing the kinesin reaction cycle with a 2D optical force clamp. Proc. Natl. Acad. Sci. U.S.A. 100, 2351-2356 (2003).
- P. Pietzonka, A. C. Barato, U. Seifert, Universal bound on the efficiency of molecular motors. J. Stat. Mech. Theory Exp **2016**, 124004 (2016).
- U. Seifert, Stochastic thermodynamics: From principles to the cost of precision. Phys. A: Stat. Mech. Appl. **504**, 176–191 (2018).
- D. D. Hackney, The tethered motor domain of a kinesin-microtubule complex catalyzes reversible synthesis of bound ATP. Proc. Natl. Acad. Sci. U.S.A. 102, 18338–18343 (2005).
- V. Bierbaum, R. Lipowsky, Chemomechanical coupling and motor cycles of myosin V. Biophys. J. 100, 1747-1755 (2011).
- W. R. Schief, R. H. Clark, A. H. Crevenna, J. Howard, Inhibition of kinesin motility by ADP and phosphate supports a hand-over-hand mechanism. Proc. Natl. Acad. Sci. U.S.A. 101, 1183-1188 (2004).
- D. Hathcock, R. Tehver, M. Hinczewski, D. Thirumalai, Myosin V executes steps of variable length via structurally constrained diffusion. *eLife* **9**, e51569 (2020).
- G. Cappello et al., Myosin V stepping mechanism. Proc. Natl. Acad. Sci. U.S.A. 104, 15328–15333 (2007).
- A. D. Mehta et al., Myosin-V is a processive actin-based motor. Nature 400, 590-593 (1999).
- C. Veigel, F. Wang, M. L. Bartoo, J. R. Sellers, J. E. Molloy, The gated gait of the processive molecular motor, myosin V. Nat. Cell Biol. 4, 59-65 (2002).
- N. M. Kad, K. M. Trybus, D. M. Warshaw, Load and Pi control flux through the branched kinetic cycle of myosin V. J. Biol. Chem. 283, 17477-17484 (2008).
- S. Uemura, H. Higuchi, A. O. Olivares, E. M. De La Cruz, S. Ishiwata, Mechanochemical coupling of two substeps in a single myosin V motor. *Nat. Struct. Mol. Biol.* **11**, 877–883 (2004).

  J. C. M. Gebhardt, A. E. M. Clemen, J. Jaud, M. Rief, Myosin-V is a mechanical ratchet. *Proc. Natl. Acad.*
- Sci. U.S.A. 103, 8680-8685 (2006).
- 76. R. D. Astumian, Kinetic asymmetry allows macromolecular catalysts to drive an information ratchet. Nat. Commun. 10, 3837 (2019).
- R. D. Astumian, I. Derényi, A chemically reversible Brownian motor: Application to kinesin and Ncd. Biophys. J. 77, 993-1002 (1999).
- R. D. Astumian, Irrelevance of the power stroke for the directionality, stopping force, and optimal efficiency of chemically driven molecular machines. *Biophys. J.* **108**, 291–303 (2015).
- R. Takaki, M. L. Mugnai, D. Thirumalai, Data for "Information flow, gating, and energetics in dimeric molecular motors." GitHub. https://github.com/kibidanngo/Information-flow-PNAS. Deposited 20 October 2022.